Design and implementation of the output feedback linearization control method to determine the DLCC of 6R manipulator

L. Alizadeh Saravi & M. H. Korayem*
Department of Engineering, Science and Research Branch,
Islamic Azad University, Tehran, Iran
E-mail: leila_alizadeh_saravi@yahoo.com & hkorayem@gmail.com
*Corresponding author

S. R. Nekoo
School of Mechanical Engineering,
Iran University of Science and Technology, Tehran, Iran
E-mail: rafee@iust.ac.ir

Received: 26 April 2014, Revised: 14 August 2014, Accepted: 20 August 2014

Abstract: In this study, feedback linearization (FL) for 6R manipulator is designed, simulated and implemented. The presented input-output FL controller has achieved the desired performance for the complicated nonlinear terms in the arm's dynamic equations. Simulations were used to test the performance of the controller for point-to-point motion as well as continuous trajectory. The results of the point-to-point motion simulations and experiments were compared, where it indicates that the proposed approach preserved smooth motion in a very short process time with good accuracy. The dynamic load carrying capacity (DLCC), which is a criterion to determine FL controller performance on 6R robot, is also investigated, based on saturated torque of the motors and allowable error bounds. Moreover, it was shown that the control law is able to accurately represent closed-loop equations and simultaneously imposed desirable behavior on 6R robot.

Keywords: 6R Robot, Inverse Kinematic, Forward Kinematic, Feedback Linearization, DLCC.

Reference: L. A. Saravi, M. H. Korayem and S. R. Nekoo, 'Design and implementation of the output feedback linearization control method to determine the DLCC of 6R manipulator', Int J of Advanced Design and Manufacturing Technology, Vol. 8/ No. 3, 2015, pp. 56-66.

Biographical notes: Leila Alizadeh Saravi received her BSc and MSc in automechanical engineering from the Khayyam Institute of Higher Education, Mashhad in 2008, and mechatronic engineering from Department of Engineering, Science and Research Branch, Islamic Azad University, Tehran in 2014, respectively. Her current research and interests include: robotics, nonlinear control, manufacturing and mechatronics systems, system dynamics and control. **M. Habibnejad Korayem** received his BSc and MSc in Mechanical Engineering from Amirkabir University of Technology in 1985 and 1987, respectively. He received his PhD in mechanical engineering from the University of Wollongong, Australia, in 1994. He is a Professor in mechanical engineering at the Iran University of Science and Technology. **Saeed Rafee Nekoo** received his BSc in mechanical engineering from Islamic Azad University, South branch, Tehran in 2007 and his MSc in mechanical engineering from Iran University of Science and Technology in 2010. He is presently a PhD student of mechanical engineering in Iran University of Science and Technology. His current research and interests include: robotics, nonlinear and optimal control, control engineering, manufacturing and mechatronics systems.

1 INTRODUCTION

Designing an appropriate robot controller is a challenging task due to its complicated nonlinear dynamics and coupling between joints. Finding a control strategy to handle a robot confidentially has a long history. Besides, implementing the prevalent linear controllers and computed torque methods, the most common control structures involve optimal controllers based on the numerical solutions to the nonlinear Hamilton-Jacobi-Bellman [1, 2] and Riccati equations [3] to minimize the cost function of the system. Uncertainty in robot modelling and the use of more complicated control methods with nonlinear structures to achieve robust designs, such as a sliding mode controller [4] and the $H_{¥}$ robust controller [5], decrease the vibration amplitude. In recent years, there is a new trend to use intelligent controllers such as genetic algorithms [6], and fuzzy controllers [7], which are non-model based methods for nonlinear systems and robots; however, their implementation is still difficult to perform.

Due to the presence of complex nonlinear terms in the dynamic equations of robots, related research trends is to use initial feedback in order to eliminate the nonlinear dynamics effects of the system and transform it to a linear form. Achieving a linear model by FL is always a focus for robot designers. The application of flexible joint manipulator is discussed in refs. [8, 9]; and concerning the flexible joint cable robot, this method is implemented as well [10]. Such a control law is also applied to biped robot for asymptotically stable periodic walking [11] which is a rich open problem [12]. Employing FL controller to improve the performance of gait rehabilitation robot is another application of such a powerful control strategy [13]. However, to the best of our knowledge most of these research efforts have not been involved experimental results.

In this study, a nonlinear FL controller for a robot with six revolute joints has been designed and implemented. The manipulator was controlled by PID algorithm [14, 15] and the SDRE controller [16]. The main contribution of this paper is to formulate input-output FL controller for the 6R robot manipulator besides investigating theoretically and experimentally the performance of the proposed controller in the presence of uncertainty (DLCC). Such a control structure practically removes the nonlinear dynamic effects and decreases coupling between the joints by transforming them into six independent linear systems.

This paper is organized as follows: Section 2 presents the FL control structure, which includes FL theory and briefly presenting the model. Simulation results are presented in Section 3 and experimental results are explained in Section 4. Section 5 reports the summary and conclusions.

2 FEEDBACK LINEARIZATION CONTROLLER DESIGN FOR 6R ROBOT

The aim of designing a nonlinear controller is to track an arbitrary desired trajectory or to regulate a desired set-point. Section 2.1 is a brief overview of input-output FL approach [17] and derives the FL control law for 6R robot.

2.1. INPUT-OUTPUT FEEDBACK LINEARIZATION CONTROL THEORY

Consider a nonlinear system described as follows:

$$\begin{aligned} \dot{x} &= f(x) + g(x)u \\ y &= h(x) \end{aligned} \tag{1}$$

where $x(t) \in \Re^n$, $u(t) \in \Re^m$ and $y(t) \in \Re^p$ are states, inputs and outputs of the system, respectively. $f(x)$, $g(x)$ and $h(x)$ assume to be the smooth functions of x with appropriate dimension. To design input-output FL controller, the output y and the control input u should be related through a linear differential equation. Since Eq. (1) indicates that the input and output of the considered system are not directly related, an explicit relationship between the input and the output is generated by successive differentiation of the output. Therefore, The i^{th} is the output derivative, and $y^{(i)}$ is derived from the Lie derivation as:

$$y^{(i)} = L_f{}^i h(x) + L_g L_f{}^{i-1} h(x) u, \tag{2}$$

where

$$L_f{}^i h(x) = L_f(L_f{}^{i-1} h(x)) = \nabla(L_f{}^{i-1} h(x))\, f(x), \tag{3}$$

$$L_g L_f{}^{i-1} h(x) = L_g(L_f{}^{i-2} h(x)) = \nabla(L_f{}^{i-2} h(x)) g(x). \tag{4}$$

In Eq. (4), $\nabla(\cdot) = \partial(\cdot)/\partial(x)$ is the Jacobi matrix and the continuous Lie derivative $L_f^0 h(x) = h(x)$. If the nonlinear system in Eq. (1) is controllable, there exists $i=r$ (r is the relative degree of the system) that for some x the following equation is satisfied:

$$L_g L_f^{r-1} h(x) \neq 0, \tag{5}$$

and the control law is in the form of:

$$u = \frac{1}{L_g L_f{}^{r-1} h(x)} (-L_f{}^r h(x) + v). \tag{6}$$

By applying the control law from Eq. (6) in Eq. (2), the linear relation is achieved as:

$$y^{(r)} = v, \tag{7}$$

where v is the new control input. For issues that require tracking of desired input (y_d), v can be defined as:

$$v = y_d^{(r)} - k_0 e - k_1 \dot{e} - k_2 \ddot{e} ... - k_{r-1} e^{(r-1)}, \tag{8}$$

where $e=y-y_d$ is the tracking error. The coefficients k_i (for $r=1,2,\ldots,r-1$) must be chosen such that all roots of the polynomial equation of error in $s^r + k_{r-1}s^{r-1} .... + k_1 s + k_0 = 0$ are placed in the left half of the complex plane.

2.2. CONTROLLER DESIGN FOR 6R ROBOT

The kinematics and dynamics of the equations for the 6R robot are shown in Fig. 1. This section considers the state space equation with the structure shown in Eq. (1):

$$\dot{X} = \begin{bmatrix} X_2 \\ -M^{-1}(X_1)[C(X_1, X_2) + G(X_1)] \end{bmatrix} + \begin{bmatrix} 0_{6\times 6} \\ M^{-1}(X_1) \end{bmatrix} U, \tag{9}$$
$$Y = \begin{bmatrix} I_{6\times 6} & 0_{6\times 6} \end{bmatrix} \begin{bmatrix} X_1 \\ X_2 \end{bmatrix},$$

Where X_1 is the state vector for angular motion and X_2 is the state vector for angular velocity. In Eq. (9), $M(X_1) \in R^{6\times 6}$ is the inertia matrix, $C(X_1, X_2) \in R^{6\times 1}$ is the centrifugal and Coriolis force, $G(X_1) \in R^{6\times 1}$ is the effect of gravity, U is the effect of torque on the rotors, and $X \in R^{12\times 1}$ is the state of the system:

$$X = \begin{bmatrix} X_1 \\ X_2 \end{bmatrix}, \tag{10}$$

where

$$X_1 = \begin{bmatrix} \theta_1 & \theta_2 & \theta_3 & \theta_4 & \theta_5 & \theta_6 \end{bmatrix}^T,$$
$$X_2 = \begin{bmatrix} \dot{\theta}_1 & \dot{\theta}_2 & \dot{\theta}_3 & \dot{\theta}_4 & \dot{\theta}_5 & \dot{\theta}_6 \end{bmatrix}^T.$$

Using FL control method from Sec. 2.1, $L_g L_f^{\,i-1} h(x)$ is calculated as:

$$\nabla h = \begin{bmatrix} I_{6\times 6} & 0_{6\times 6} \end{bmatrix} \Rightarrow L_g h(x) = 0_{6\times 1}; i = 1, \tag{11}$$
$$L_f h(x) = X_2 \Rightarrow L_g L_f h(x) = M^{-1}(X_1); i = 2. \tag{12}$$

Since $L_g L_f h(x) \neq 0$, the relative degree of the system is 2 ($r=2$). By substituting Eq. (6), the FL control law for 6R robot is achieved by following relation:

$$U = \frac{1}{L_g L_f^{\,1} h(x)} (L_f^{\,2} h(x) + V), \tag{13}$$

where $V = \ddot{Y} \in R^{6\times 1}$ is the new input vector and:

$$\nabla(L_f h(x)) = \begin{bmatrix} 0_{6\times 6} & I_{6\times 6} \end{bmatrix}$$
$$\Rightarrow L_f^{\,2} h(x) = -M^{-1}(X_1)[C(X_1, X_2) + G(X_1)], \tag{14}$$

$$L_g L_f h(x) = M^{-1}(X_1). \tag{15}$$

The input control of FL control law is achieved by:

$$U = M(X_1)V + C(X_1, X_2) + G(X_1). \tag{16}$$

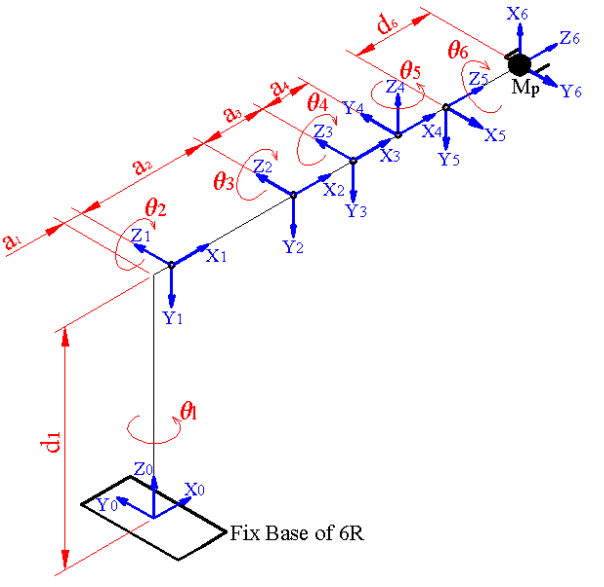

Fig. 1 6R manipulator [1]

By applying input-output FL control law in Eq. (16) to the robot system of Eq. (9), the robot state-space equations are converted to the following linear form:

$$\dot{X} = \begin{bmatrix} 0_{6\times 6} & I_{6\times 6} \\ 0_{6\times 6} & 0_{6\times 6} \end{bmatrix} X + \begin{bmatrix} 0_{6\times 6} \\ I_{6\times 6} \end{bmatrix} V, \tag{17}$$
$$Y = \begin{bmatrix} I_{6\times 6} & 0_{6\times 6} \end{bmatrix} X. \tag{18}$$

According to the linear state-space equation for the structure of the robot, each input is applied to a joint by a second-order differential equation and the overall robot process can be described by 6 decoupled subsystems. Therefore, there is not any unobserved internal dynamics, although the robot has 12 state variables. New input v can be produced by the following equation to achieve good tracking for each joint of the robot:

$$v_i = \ddot{y}_{id} - k_{id}\dot{e}_i - k_{ip} e_i; i = 1, 2...6, \tag{19}$$

where $y_{id}=\theta_{id}$ is the desired angle of the i^{th} joint and $e_i = y_i - y_{id}$ is the tracking error of the i^{th} joint. The structure of the proposed closed-loop 6R robot is shown

in Fig. 2 where $\Theta_d \in R^{6\times1}$ and Θ are the vector of the desired path and the joint angles of the robot, respectively.

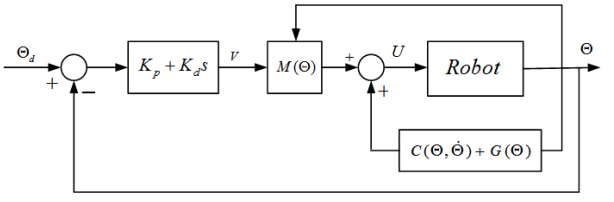

Fig. 2 FL control loop for 6R robot

In this section, a suitable design for a nonlinear controller based on input-output feedback linearization was carried out to achieve the desired performance and proper tracking of the robot. In the next section, the accuracy of design is examined using simulations and experiments.

3 SIMULATION OF FEEDBACK LINEARIZATION CONTROL METHOD

This section investigates the simulation results of FL control for point-to-point motion and trajectory tracking problems.

3.1. POINT TO POINT MOTION

Let us consider P_i(0.3501,0.5119,0.6501) and P_f(0.5253,–0.3212,0.3092) as the initial and end points, respectively. Using inverse kinematics relations, the desired joint angles for the initial and final points are:

$$\Theta_{id} = [0.9534 \quad -0.3611 \quad 0.03140 \quad -0.0157 \quad -1.4994 \quad 0.0233]^T \tag{20}$$

$$\Theta_{fd} = [-0.6623 \quad 0.0942 \quad 0.5652 \quad -0.5338 \quad -1.0965 \quad 0.3954]^T \tag{21}$$

The robot dynamic load carrying capacity is determined, beginning with an initial value for load m_p and increasing it step-by-step until the system error remained in acceptable bound. Under actual and laboratory conditions, the limited applied torque to each link is restricted using the following equations:

$$U_{\max} = U_s - \frac{U_s}{\omega_s}\omega \tag{22}$$

$$U_{\min} = -U_s - \frac{U_s}{\omega_s}\omega \tag{23}$$

in which U_{max} and U_{min} are the maximum and minimum stall torques of the joints, respectively; ω is the joint angular velocity; U_s and ω_s are the saturated torque of the motor and no-load speed of the motor (Table 1). The flowchart in Fig. 3 shows the simulation steps of FL controller for point-to-point motion.

Table 1 Motor Characteristics [14]

Joint	$U_s(N.m)$	$\omega_s(rad/s)$
1	114	1.32
2	98	1.04
3	382.2	0.73
4	40.4	9.01
5	40.4	9.01
6	40.4	9.01

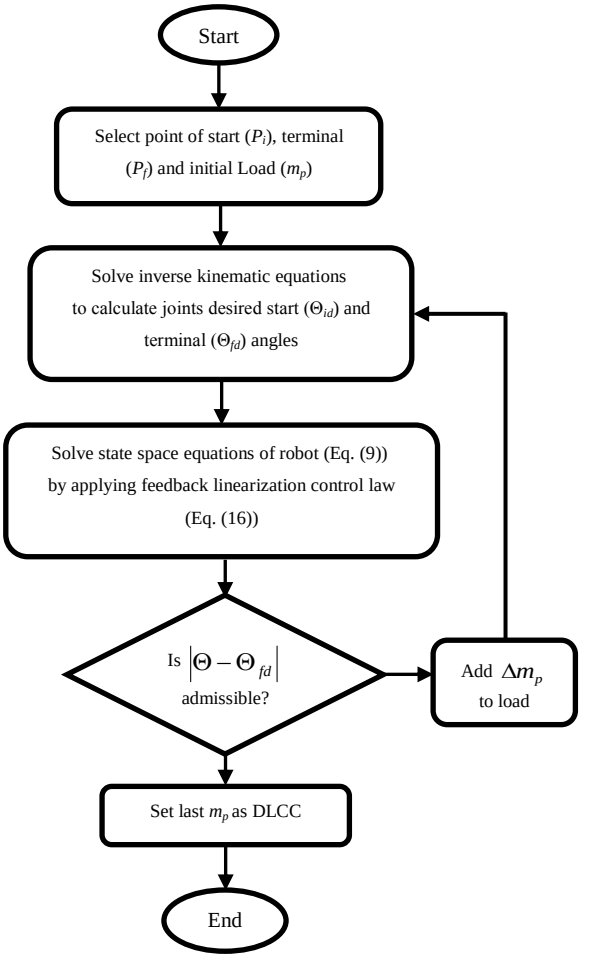

Fig. 3 Flowchart of FL for point-to-point motion

The simulation time for point-to-point motion is assumed to be 4.5s. Figs. 4 and 5 show the robot path from the initial point to the end point and the torques applied to the robot joints, respectively.

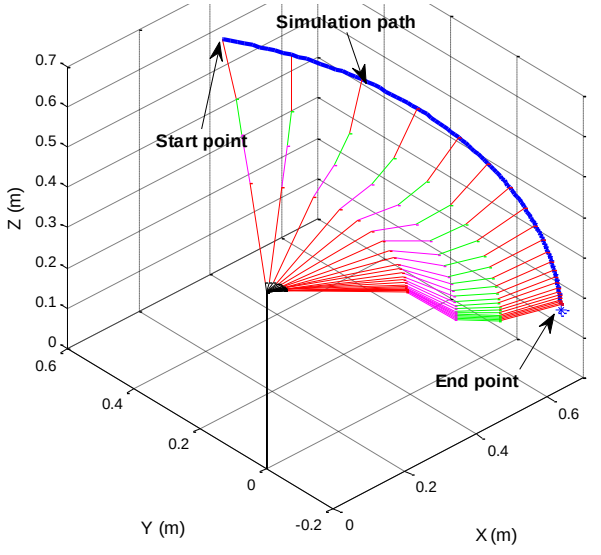

Fig. 4 Path of end-effector from the initial point to end point

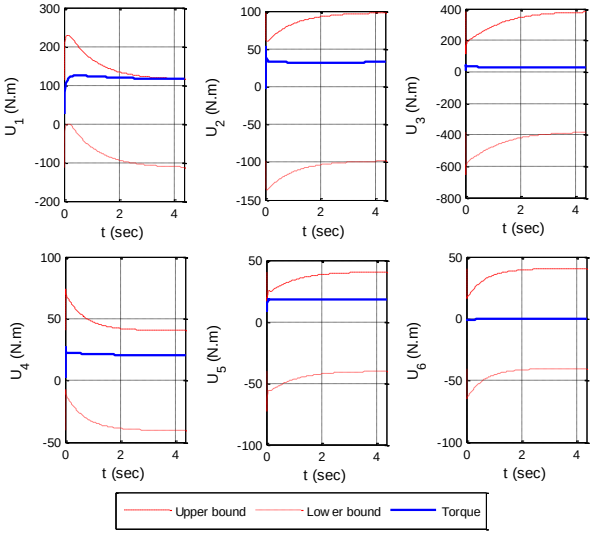

Fig. 5 Torque applied to joints in point-to-point motion

Figure 4 demonstrates that the design has led to continuity and smoothness of the robot joint angles (a goal of the design) and that the robot has reached the end point with good accuracy. The torque applied to the joints for point-to-point motion was within the calculated range (Fig. 5) and the maximum dynamic load carrying capacity was 660g (assuming 10 mm maximum error in end-effector).

3.2. CIRCULAR TRAJECTORY TRACKING

A circular path is defined for end-effector movement to test and verify the operation of FL tracking control. The simulation time for circular motion is assumed $t_f=2\pi$ seconds and m_p = 0.3 kg is the load. In this part both maximum allowable torque and maximum allowable error were regarded for simulation. In the first case, controller coefficients are chosen in such a way to avoid saturation. In the second case, maximum error (e_{max}) is assumed to be less than 10mm; to decrease error, larger values for the proportional and derivative coefficients of the controller were selected.

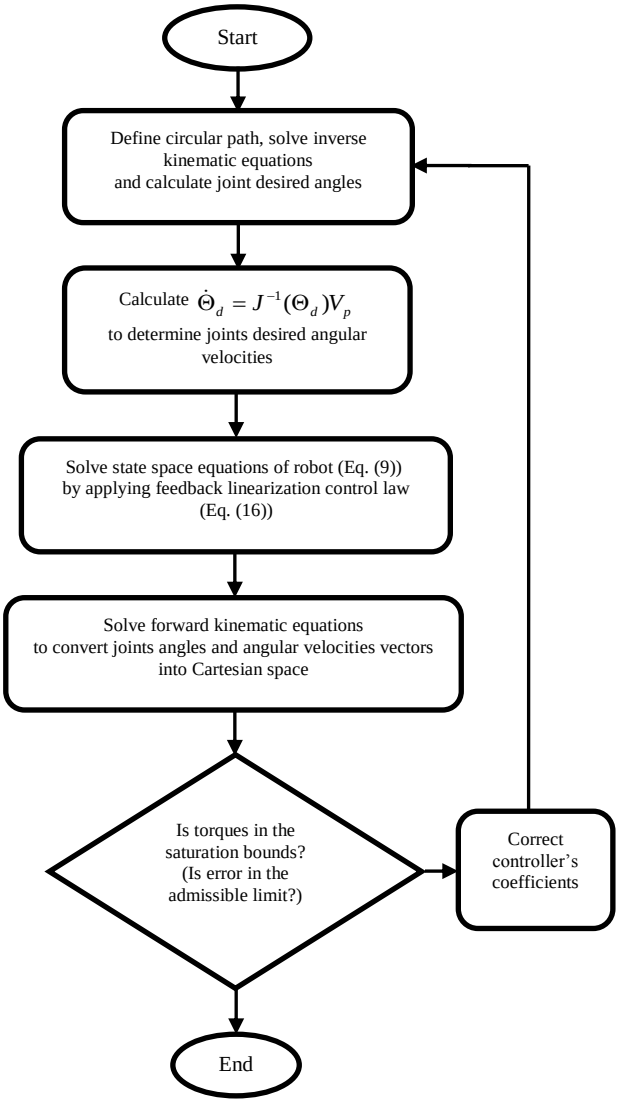

Fig. 6 Flowchart of FL for maximum permitted torque (error) in circular motion

The flowchart of design process and simulation for maximum allowable torque and error are shown in Fig. 6, where $V_d = [\dot{p}_{xd} \quad \dot{p}_{yd} \quad \dot{p}_{zd}]^T$ is the desired Cartesian velocity vector and $J(\Theta_d)$ is the Jacobian matrix corresponding to the desired joint angles for the robot.

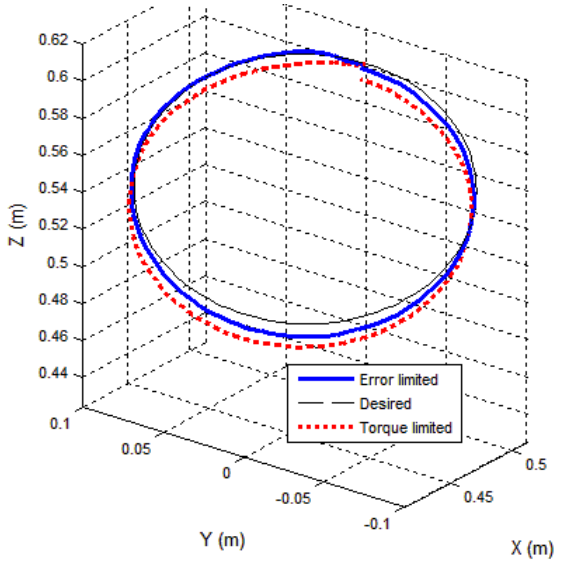

Fig. 7 End-effector motion in a circular path for maximum permitted error and torque

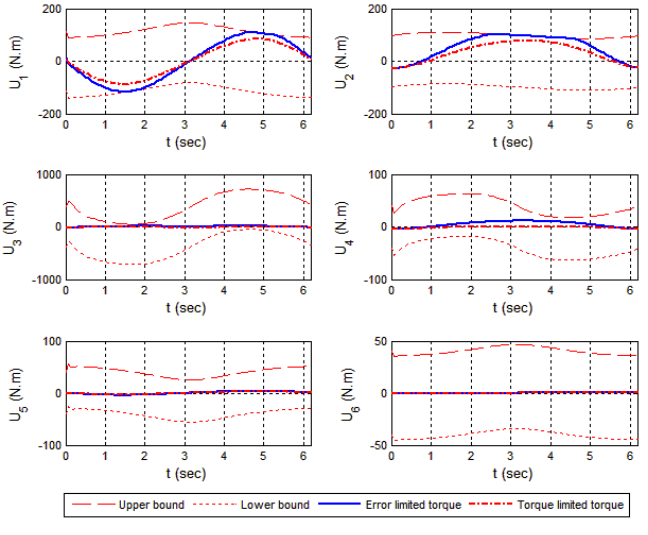

Fig. 8 Motor torque in a circular path for maximum permitted error and torque

To decrease error and achieve better accuracy in the maximum permitted error simulation, larger coefficients were determined for the controller. As a result, torques were exceeded the maximum permitted bound. The tracking error was calculated as in Eq. (24):

$$e(t) = \sqrt{(x_d(t) - x(t))^2 + (y_d(t) - y(t))^2 + (z_d(t) - z(t))^2}, \quad (24)$$

where $e(t)$ is the tracking error, $[x_d(t) \quad y_d(t) \quad z_d(t)]^T$ are the desired Cartesian coordinate vectors, and $[x(t) \quad y(t) \quad z(t)]^T$ are the coordinates of the end-effector (Fig. 9).

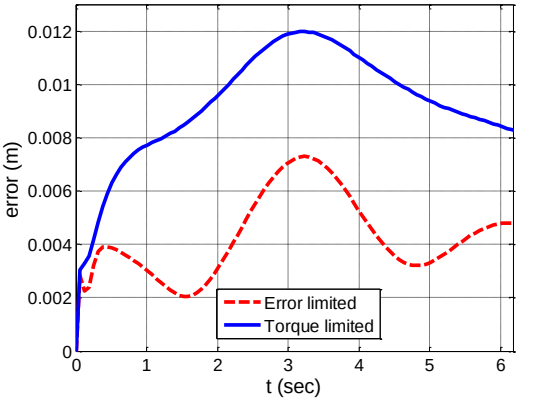

Fig. 9 Motor torque in a circular path for maximum permitted error and torque

As it was shown in Fig. 9, the end-effector for the second case (maximum permitted error) allowed $E_{\max}(t)\big|_{t=3.23} = 7.3\,\text{mm}$ which was in the specified 10 mm range and the design showed better accuracy than for the first case (maximum permitted torque). The penalty for achieving high accuracy was the use of greater control signals and generating greater driving torques. An appropriate design should be a compromise of these two issues (precision and limits of actuator signal).

Fig. 10 6R robot manipulator [14]

4 IMPLEMENTATION OF FEEDBACK LINEARIZATION CONTROL ON 6R ROBOT

The algorithm in Fig. 3 was used to implement the FL control on the 6R robot (Fig. 10) for $t \in (0,4.34)s$. The results are shown in Figs. 11 and 12 for joint angle variations and trajectory of the end-effector from the initial point to the end point, respectively.

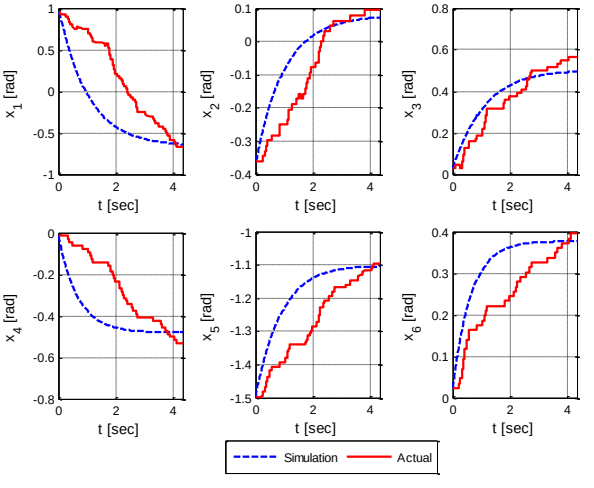

Fig. 11 Angular positions of links for simulation and experiment

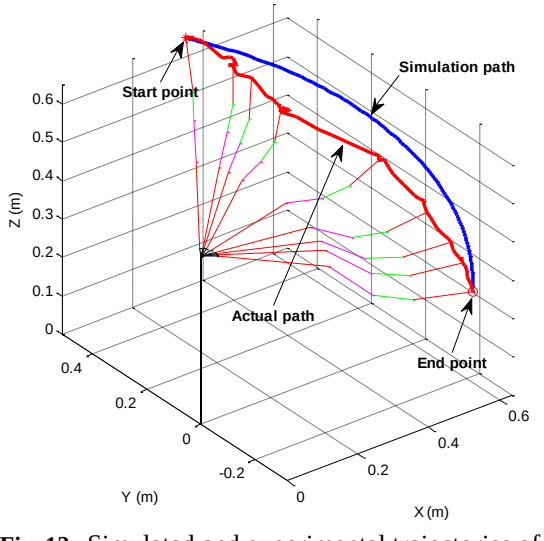

Fig. 12 Simulated and experimental trajectories of end-effector

Figures 11 and 12 confirmed that, the result of practical implementation of FL has provided good performance; despite the differences between the results of the simulation and the experiments, the robot eventually reached the end point (target).

5 CONCLUSION

In the present study, a FL approach for 6R robot is designed, simulated and implemented to improve tracking performance. FL control removed the nonlinear terms of the robot, eliminated interference between the dynamics of the joints, and created a simple structure for the robot. Simulating point-to-point motion and tracking in a circular path allowed evaluation of the performance of the proposed design. For point-to-point motion, by selecting an initial value for the load and determining the proportional-derivative coefficients of the controller, the load was enhanced to achieve acceptable system error and the torques applied to the joints did not reach the saturation bound.

The simulation results showed that the FL controller performed appropriately to achieve the target in the presence of an uncertain dynamic load. For a circular trajectory, choosing large values for the proportional derivative coefficients of the controller decreased the error rate for a specified load to any desired level, saturating the driving torques. The best tracking and performance is a compromise between the torques and error limitations. The simulations showed smooth motion, no-chattering and high precision along with good tracking of the robot in a continuous path. It can be practically implemented and the simulation results indicated that the performance of the robot achieved the target using point-to-point motion.

REFERENCES

[1] Korayem, M. H., Irani, M., and Nekoo, S. R., "Analysis of Manipulators using SDRE: A Closed Loop Nonlinear Optimal Control Approach", Journal of Sciatica Iranica, Transaction B: Mechanical Engineering, Vol. 17, No. 6, 2010, pp. 456-467.

[2] Korayem, M. H., Irani, M., and Nekoo, S. R., "Motion Control and Dynamic Load Carrying Capacity of Mobile Robot via Nonlinear Optimal Feedback", AMAE International Journal on Manufacturing and Material Science, Vol. 2, No. 1, 2012, pp. 16-21.

[3] Korayem, M. H., Irani, M., and Nekoo, S. R., "Load Maximization of Flexible Joint Mechanical Manipulator using Nonlinear Optimal Controller", Acta Astronautica, Vol. 69, No. 7, 2011, pp. 458-469.

[4] Majidabad, S. S., Shandiz, H. T., "Discrete-time Based Sliding Mode Control of Robot Manipulators", International Journal of Intelligent Computing and Cybernetics, Vol. 5, No. 3, 2012, pp. 340-358.

[5] Zhang B. L., Ma, L., and Han, Q. L., "Sliding Mode H∞ Control for Offshore Steel Jacket Platforms Subject to Nonlinear Self-Excited Wave Force and External Disturbance", Nonlinear Analysis: Real World Applications, Vol. 14, No. 1, 2013, pp. 163-178.

[6] Koker, R., "A Genetic Algorithm Approach to a Neural-Network-Based Inverse Kinematics Solution of Robotic Manipulators Based on Error Minimization", Information Sciences, Vol. 222, 2013, pp. 528-543.

[7] Bachir, O., Zoubir, A. F., "Adaptive Neuro-fuzzy Inference System Based Control of Puma 600 Robot Manipulator", International Journal of Electrical and Computer Engineering, Vol. 2, No. 1, 2012, pp. 90-97.

[8] Korayem, M. H., Davarpanah, F, and Ghariblu, H., "Load Carrying Capacity of Flexible Joint Manipulators with Feedback Linearization", International Journal of Advanced Manufacturing Technology, Vol. 29, No. 3-4, 2006, pp. 389-397.

[9] Korayem, M. H., Firouzy, S., and Heidari, A., "Dynamic Load Carrying Capacity of Mobile-base Flexible-link Manipulators: Feedback Linearization Control Approach", IEEE International Conference on Robotics and Biomimetics, China, Dec. 2007, pp. 2172-2177.

[10] Korayem, M. H., Tourajizadeh, H., and Bamdad, M., "Dynamic Load Carrying Capacity of Flexible Cable Suspended Robot: Robust Feedback Linearization Control Approach", Journal of Intelligent & Robotic Systems, Vol. 60, No. 3-4, 2010, pp. 341-363.

[11] Hu, Y., Yan, G., and Lin, Z., "Feedback Control of Planar Biped Robot With Regulable Step Length and Walking Speed", IEEE Transactions on Robotics, Vol. 27, No. 1, 2011, pp. 162-169.

[12] Grizzle, J. W., Chevallereau, C., Sinnet, R. W., and Ames, A. D., "Models, Feedback Control, and Open Problems of 3D Bipedal Robotic Walking", Automatica, Vol. 50, No. 8, 2014, pp. 1955-1988.

[13] Chisholm, K. J., Klumper, K., Mullins, A., and Ahmadi, M., "A Task Oriented Haptic Gait Rehabilitation Robot", Mechatronics, 2014, (Article in Press).

[14] Korayem, M. H., Nekoo, S. R., and Abdollahi, F., "Hardware Implementation of a Closed Loop Controller on 6R Robot using ARM Microcontroller", International Research Journal of Applied and Basic Sciences, Vol. 4, No. 8, 2013, pp. 2147-2158.

[15] Korayem, M. H., Irani, M., and Nekoo, S. R., "Application of Stereo Vision and ARM Processor for Motion Control", in Interdisciplinary Mechatronics (eds M. K. Habib and J. P. Davim), John Wiley & Sons, Inc., Hoboken, NJ USA, 2013. doi: 10.1002/9781118577516.ch18.

[16] Korayem, M. H., Nekoo, S. R., "Finite-time State-dependent Riccati Equation for Time-varying Nonaffine Systems: Rigid and Flexible Joint Manipulator Control", ISA Transactions, Vol. 54, 2015, pp. 125-144.

[17] Slotine, J. J. E., Li, W., "Applied Nonlinear Control", Prentice Hall, 1991.